Taylor & Francis
Taylor & Francis Group

Architectural Engineering and Design Management

ISSN: (Print) (Online) Journal homepage: https://www.tandfonline.com/loi/taem20

Impact of building envelope parameters on occupants' thermal comfort and energy use in courtyard houses

Hoorieh Ghorbani Naeini, Alireza Norouziasas, Farimah Piraei, Maryam Kazemi, Mostafa Kazemi & Mohamed Hamdy

To cite this article: Hoorieh Ghorbani Naeini, Alireza Norouziasas, Farimah Piraei, Maryam Kazemi, Mostafa Kazemi & Mohamed Hamdy (2023): Impact of building envelope parameters on occupants' thermal comfort and energy use in courtyard houses, Architectural Engineering and Design Management, DOI: 10.1080/17452007.2023.2254294

To link to this article: https://doi.org/10.1080/17452007.2023.2254294

Published online: 02 Sep 2023.

ARCHITECTURAL ENGINEERING AND DESIGN MANAGEMENT
https://doi.org/10.1080/17452007.2023.2254294

Impact of building envelope parameters on occupants' thermal comfort and energy use in courtyard houses

Hoorieh Ghorbani Naeini[a], Alireza Norouziasas[b], Farimah Piraei[c], Maryam Kazemi[d], Mostafa Kazemi[e] and Mohamed Hamdy[b]

[a]Faculty of Architecture, College of Fine Arts, University of Tehran, Tehran, Iran; [b]Department of Civil and Environmental Engineering, Norwegian University of Science and Technology, Trondheim, Norway; [c]Department of Energy 'Galileo Ferraris', Politecnico di Torino, Torino, Italy; [d]Faculty of Architecture and Urban Planning, Qazvin Islamic Azad University, Qazvin, Iran; [e]GeMMe Building Materials, Department of Urban and Environmental Engineering (UEE), University of Liège, Liège, Belgium

ABSTRACT

Courtyard houses constructed recently with air-conditioning systems need to increase efficiency by simultaneously reducing thermal load and improving thermal comfort in all seasonal zones around the yard. The envelope design is one of the effective parameters in reducing energy consumption and increasing thermal comfort. Therefore, this study investigated the effect of some design parameters related to the envelope of the building on Predicted Mean Vote (PMV) and thermal loads. The design parameters were Wall Construction (WLC) and Window Construction (WID) with different U-values (thermal transmittance), Window to Wall Ratio (WWR), Depth of Shading (DSH), and the Number of Shading (NSH). This research proposed a parametric study process that can simultaneously help designers evaluate the PMV values and thermal loads of numerous design options in four seasonal zones around the courtyard and generate optimized design solutions. According to the results, the PMV of best design solution (BS) compared with the worst design solution (WS) increased by 8%, 9%, 8%, and 12% in different zones. The thermal load decreased by 21%, 26%, 22%, and 21%. According to the sensitivity analysis, PMV values for most zones were negatively affected (decreased) by WID.

ARTICLE HISTORY
Received 14 December 2022
Accepted 26 August 2023

KEYWORDS
Predicted mean vote; courtyard houses; thermal load; wall construction; thermal comfort

Nomenclature

WWR	Window to Wall Ratio
WLC	Wall Construction
WID	Window Construction
BS	Best design Solution
WS	Worst design Solution
PMV	Predicted Mean Vote
PPD	Percent of People Dissatisfied
SRC	Standard Regression Coefficient
USRC	Un standard Regression Coefficient
EPW	Energy Plus Weather Data
EP	Energy Plus
RC	Real Case
NSH	Number of Shading

CONTACT Mostafa Kazemi mostafa.kazemi@uliege.be

DSH	Depth of Shading
MRT	Mean Radiant Temperature
AT	Air Temperature
RH	Relative Humidity
HVAC	Heating, Ventilating and Air Conditioning
U-value	Thermal transmittance

Introduction

The construction sector is considered one of the most cost-effective areas to decrease energy consumption in building industries (Alkalbani, Rezgui, Vorakulpipat, & Wilson, 2013; Bhatnagar et al., 2022; Kazemi & Courard, 2021a; Kazemi, Courard, & Hubert, 2022; Lee, Kim, Song, Kim, & Jang, 2017; Norouziasas et al., 2023; Rahif, Kazemi, & Attia, 2023; Thanu, Rajasekaran, & Deepak, 2023). Also, residential building leads to around 70% of energy consumption in developing countries (Manzano-Agugliaro, Montoya, Sabio-Ortega, & García-Cruz, 2015; Safizadeh, 2023). One of the most critical requirements of the building is to provide thermal comfort for occupants. Based on the ASHRAE definition, thermal comfort is a state of mind that expresses a sense of satisfaction with the thermal environment (Ashrae, 2004). Since individual thermal comfort depends on personal and environmental parameters (Efeoma & Uduku, 2014; Jaffal, Inard, Ghaddar, & Ghali, 2020; Sharma & Kumar, 2023), analyzing thermal comfort is difficult (Ghaffour, Ouissi, & Velay Dabat, 2020). Personal parameters include people's level of activity and clothing within a built environment, and environmental parameters are the airflow, mean radiant temperature of surfaces, air temperature, and humidity rate (Taleghani, 2018).

The envelope is in direct contact with the external environment, and an average of 75% of the heat loss/gain occurs in the building envelope (Aydın & Mıhlayanlar, 2020). Indeed, one of the most crucial elements in defining a building's energy efficiency might be considered to be the façade design and the thermophysical properties of the materials used (Kazemi, Courard, & Attia, 2023; Kazemi, Courard, & Hubert, 2021; Madandoust, Bazkiyaei, & Kazemi, 2018; Mirrahimi et al., 2016; Moein et al., 2023). For instance, lowering the U-value enhances thermal performance, which can be attained using a various techniques depending on the climate, including adding more glazing layers, using special coatings to control solar radiation, and filling gaps between two layers with low thermal conductive gases (Al-Saadi, 2006; Carmody, Selkowitz, Lee, Arasteh, & Willmert, 2004; Norouziasas, Pilehchi Ha, Ahmadi, & Rijal, 2022; Piraei, Matusiak, & Lo Verso, 2022; Rahif et al., 2022). Also, the window is one of the most critical parts of the building, responsible for about 60% of the total energy loss of a building (Jelle et al., 2012). Using windows with low thermal transmittance can significantly lower building energy expenses and result in significant energy savings (Cuce & Riffat, 2015; Javed, Ørnes, Myrup, & Dokka, 2019; Nigra, Lo Verso, Robiglio, Pellegrino, & Martina, 2022). Therefore, choosing an appropriate design strategy for the envelope, including the U-value of Wall Construction (WLC), U-value of Window Construction (WID), and shading characteristics, is essential to enhance the energy efficiency of contemporary construction (Hinkle, Wang, & Brown, 2022; Kishore, Bianchi, Booten, Vidal, & Jackson, 2021). Moreover, a unique feature of citizens' apartments is the arrangement of small-scale complexes in straight-line buildings. Small-scale buildings suffer from a lack of consideration based on environmental conditions. These buildings can include a courtyard as already used for Hyundai Ahyeon and Namahyeon apartments in Korea (Jang & Ham, 2017). Although the courtyard houses have practical climate-responsive merits, they have received less attention in current designs (Fathy, 2014; Pilechiha, Norouziasas, Ghorbani Naeini, & Jolma, 2021; Teshnehdel, Soflaei, & Shokouhian, 2020; Yilmaz & Donaldson, 2005).

To predict thermal sensation for a group of people from the human thermal load, the most popular index is Predicted Mean Vote (PMV) (Fanger, 1972). Moreover, it has been well recognized by thermal comfort standards (Carlucci, Bai, de Dear, & Yang, 2018). Considering this, plenty of research works have used PMV index to measure the thermal comfort of indoor spaces, (De Dear,

Kim, Candido, & Deuble, 2015; Enescu, 2017; Ghaffour et al., 2020; Pourshaghaghy & Omidvari, 2012). This index was developed by Fanger (Fanger, 1972). Therefore, there is a need to present a method based on the parametric study for a courtyard house to achieve a desired value of PMV and decrease the thermal load in all seasonal zones around the courtyard by selecting the most suitable wall, window construction, and shading design.

Under the climate of Cyprus, Kalogirou et al. (Kalogirou, Florides, & Tassou, 2002) investigated the effect of the thermal mass of WLC on cooling and heating load by modeling and simulation tools. The simulation results revealed that 47% of the heating load decreased by applying thermal mass, reducing diurnal temperature fluctuation. By contrast, other researchers (Zhou, Zhang, Lin, & Li, 2008) demonstrated that the cooling load increased slightly by adding thermal mass and night ventilation. Besides, Gregory et al. (Gregory, Moghtaderi, Sugo, & Page, 2008) showed that the thermal wave was delayed and flattened by a massive thermal mass in the exterior wall. Moreover, the thermal mass reduced temperature swing and stored the added internal heating and solar gain. Furthermore, De Rubies et al. (de Rubeis, Nardi, Ambrosini, & Paoletti, 2018) concluded that using the material with a high U-value increased the heat loss, resulting in low energy efficiency for building envelopes. Under the climate of Istanbul, Fernandes et al. (Fernandes, Rodrigues, Gaspar, Costa, & Gomes, 2019) demonstrated that lightweight materials with a higher U-value reduced energy consumption. For example, light thermal mass with high thermal transmittance had a better performance in energy consumption in the same climate zone. In contrast, heavyweight construction increased the cooling energy demand and reduced the heating energy demand for the southern and warmer climates. Reilly and Kinnane (Reilly & Kinnane, 2017) showed that the high thermal mass was effective in hot and arid climates. However, the high thermal mass in a cold climate was not positive, meaning the energy consumption increased by applying thermal mass in a cold climate.

Under the hot arid regions climate of the United States (BWh climate), Soflaei et al. (Soflaei, Shokouhian, Tabadkani, Moslehi, & Berardi, 2020) indicated that the effect of material type was more important than window type, and the highest thermal comfort in this research, around 38%, was for the courtyard with a height of (9 m). In addition, the height of the courtyard's walls was more influential in increasing the adaptive thermal comfort than those of width and length (Soflaei et al., 2020). Under four major climatic regions of China, Zhao and Du (Zhao & Du, 2020) showed that proper Window-to-Wall Ratio (WWR) and shading shape achieved optimal design solutions. In Tianjin, Shanghai, and Guangzhou, discomfort hours decreased by 2.53%, 0.81%, and 1.74%, respectively, and the total energy consumption decreased by 8.08%, 11.70%, and 26.70%, respectively. Under the 3B climate (cold semi-arid climate), Bakmohammadi and Noorzai (Bakmohammadi & Noorzai, 2020) showed that considerable effect on the cooling and heating energy consumption was for the WWR. Also, it was proven that the orientation of 0° had the best performance. In other words, the building with a southern window showed a good thermal comfort performance. Under Shiraz's hot arid climate in Iran, Pilechiha et al. (Pilechiha et al., 2021) found that indoor thermal comfort was 8.3% higher in winter than in the summer in the seasonal zones. In northern zones with southern windows, the seasonal movement of occupants improved the indoor thermal comfort from 10.1 to 23.7%. The improvement in southern zones with north windows increased slightly from 2.2 to 4.8%.

Based on the literature review, it is evident that certain research on the effect of design parameters on thermal load and comfort has been done. Also, it is known that courtyards are effective at controlling bioclimate, especially in hot, arid areas (Fathy, 2014; Soflaei et al., 2020). Due to a need for energy efficiency improvements, some studies have been done to enhance the design efficiency of courtyard houses in subtropical desert climates (Soflaei et al., 2020). However, there was a gap in improving thermal comfort by considering different design parameters altogether including the WWR, WID, and WLC with different U-values, Depth of Shading (DSH), and Number of Shading (NSH) multi-zone houses to analyze the PMV value and thermal load simultaneously in all zones around the courtyard. Therefore, considering the aforementioned design parameters

altogether, the main objective of this study was to reveal a method based on a parametric study to increase thermal comfort and decrease energy consumption in northern, eastern, southern, and western zones around the courtyard houses under the hot arid climate of Tehran city, Iran. The PMV value and thermal load of the Real Case (RC), Best design Solution (BS), and Worst design Solution (WS) were compared. The best design solution for each zone was proposed and the relationship between design parameters of all seasonal zones was assessed by conducting a sensitivity analysis.

Methodology

Conceptual study framework

In the first step, to build the parametric model, a courtyard house with four zones in Tehran was considered and the effective design parameters (independent variables) on the PMV value and thermal load were selected based on previous studies (Hinkle et al., 2022; Kishore et al., 2021; Soflaei et al., 2020; Zhao & Du, 2020). The model for simulation purposes was created by Rhinoceros software and the Grasshopper (Grasshopper, 2021). In the second step, the simulations of energy consumption and calculating thermal comfort were conducted by Ladybug and Honeybee (Roudsari & Pak, 2013) to obtain PMV value and thermal load. The process of parametric study was set in the third step, and the optimal design solutions were achieved. In this phase, the Design Explorer (Brown, Jusiega, & Mueller, 2020) was used to visualize the candidates and how the design parameters affected the objectives: PMV value and thermal load (dependent variables). In the fourth step, the relationship between the design parameters and objectives was found by means of Standard Regression Coefficient (SRC) analysis. In the last step, the data analysis by Python was used in the discussion to show the research summary. Also, the correlation of measured and simulated PMV values was analyzed for each zone. The research framework is shown in Figure 1.

Design parameters (independent variables)

Design parameters of this research were WWR of all zones, WLC and WID U-value, DSH, and NSH, which can be seen in Table 1. These parameters can affect the PMV value and thermal load as revealed by other researchers (Hinkle et al., 2022; Kishore et al., 2021; Soflaei et al., 2020; Zhao & Du, 2020). The WWR had two distinct 50% and 70%. The shading systems in this study were considered as fixed horizontal louvers. The number and depth of shading were the number of depth of blades. Considering this, the number of shading was 4 and 6, the depth of shading was 0.3 and 0.5 m, and the WLC and WID with different U-values were other variables.

WLCs and WIDs

As for the WLC, based on Table 2, four WLCs with different U-values based on what was prevalent in Iran were defined according to Handbook Fundamental ASHRAE, 2017 (ASHRAE, 2017). All wall construction had the same insulation and finishing layers. Expanded polystyrene (EPS) was considered as the insulation layer of all wall constructions. The first core structure to create the first wall construction was core1 with the least density of 464–512 Kg/m^3 and thermal conductivity around 0.29 W/m.K.

Table 1. Design parameters.

Design parameters	Range	Description
WWR of all zones	50% or 70%	The height of all windows is 1.8 m, the sill is 0.6 m
V2-WLC	U-value 0.6–0.93 (W/m^2 K)	Four different WLCs are defined
V3-WID	U-value 1.99–3.86 (W/m^2 K)	Four different WIDs are defined
V4-DSH (m)	0.3–0.5(m)	–
V5-NSH	4–6	–

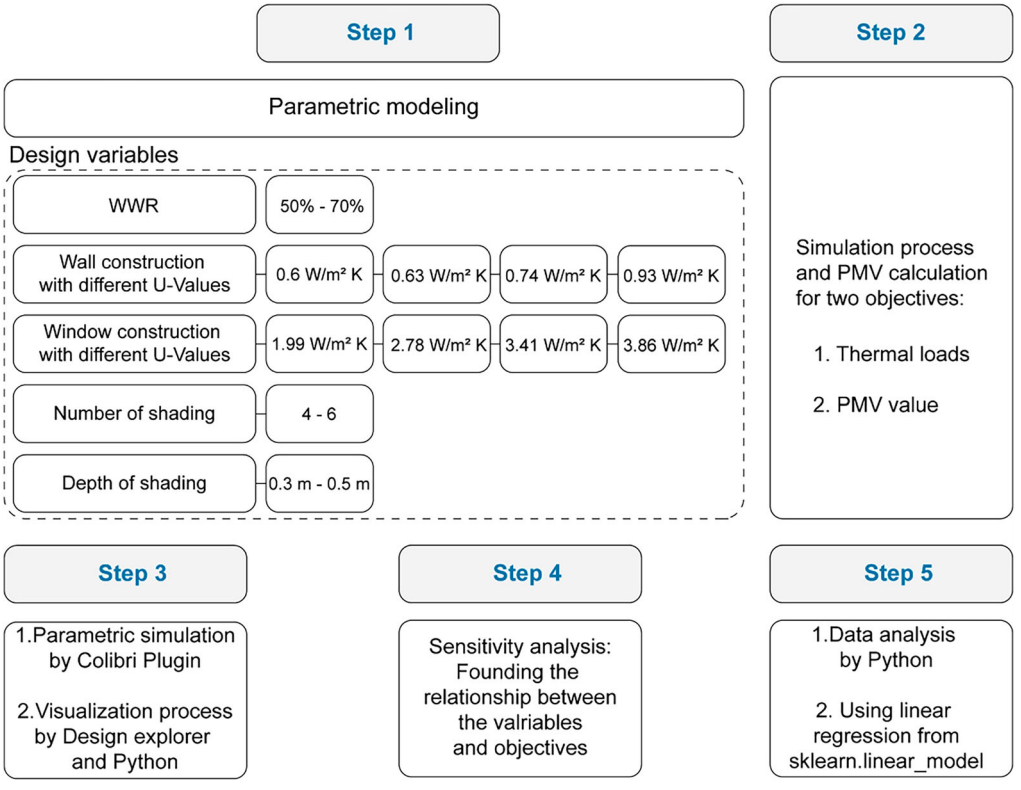

Figure 1. Conceptual study framework.

The specific heat of this core was 880 J/(kg·K). Core 2 had thermal conductivity of 0.33 W/m.K, and the density of 1390 Kg/m^3. Its specific heat was 880 J/(kg·K). Moreover, the core3 had thermal conductivity of 0.53 W/m.K. Its density and specific heat capacity were 1280 Kg/m^3 and 840 J/(kg·K),

Table 2. Thermal properties of prevalent WLCs.

Wall construction	Layers of wall construction	Thermal Conductivity (W/m.K)	Density (Kg/m^3)	Specific Heat (J/(kg·K))	Thickness (m)	U-value for different thicknesses (W/m^{2}K)
WLC1	Cement Plaster	0.72	1860	840	0.01	0.6
	Core1	0.29	512-464	880	0.2	
	EPS	0.034	24	1210	0.025	
	Cement Plaster	0.72	1860	840	0.01	
WLC2	Cement Plaster	0.72	1860	840	0.01	0.67
	Core2	0.33	1390	880	0.2	
	EPS	0.034	24	1210	0.025	
	Cement Plaster	0.72	1860	840	0.01	
WLC3	Cement Plaster	0.72	1860	840	0.01	0.74
	Core3	0.53	1280	840	0.2	
	EPS	0.034	24	1210	0.025	
	Cement Plaster	0.72	1860	840	0.01	
WLC4	Cement Plaster	0.72	1860	840	0.01	0.93
	Core4	1.95	2240	900	0.2	
	EPS	0.034	24	1210	0.025	
	Cement Plaster	0.72	1860	840	0.01	

respectively. The core 4 had the highest thermal conductivity, density, and specific heat capacity about 1.95 W/m.K, 2240 Kg/m^3 and 900 J/(kg·K), respectively. The only parameter used to compare the WLCs was U-value. Table 3 shows that different WIDs variables were listed based on the 3B climate zone following the climate of Tehran. The U-value of WIDs was selected based on the ASHRAE standard 90 (ANSI/ASHRAE Standard 90.1, 2019) for each window.

Case study building and site climate

The courtyard house was a prevalent passive design strategy used in Iran (Talebian, 2018). As shown in Figure 2, the chosen case study was a widespread courtyard house with four zones and it was located in Tehran, Iran (35°40′56.7″N, 51°25′25.5″E). The real building as the real case (RC) had a WWR of 50%, the wall and window constructions were WLC4 and WID4 with the highest U-value, and the number and depth of shading were 4 and 0.3 m, respectively.

According to the Koppen Climate Classification (BSk), Tehran has a cold semi-arid climate (Meteorological Organization Country, 2020). Tehran's relative humidity, dry bulb temperature, and wind speed are depicted in Figure 3. The least relative humidity was for March and the highest relative humidity was for December, as for the dry bulb temperature, the least and highest dry bulb temperatures were for the December and August, respectively. The highest wind speed was between October and November and, the least wind speed was in August.

Modeling

The simulated model and related dimensions are shown in Figure 4. Each zone had an area of 50 m^2, and the height of all zones was 3 m. The window height was considered 1.8 m, and the height from floor to window was 0.6 m. The model had four zones located in the north, east, west, and south, consequently, the model consisted of zones with southern, western, northern, and eastern windows, respectively. In this parametric study, two variables were the depth and number of shading. The shading depth and number, the WWR, WLC, and WID were assigned parametrically by using Rhinoceros software and the Grasshopper plugin (Grasshopper, 2021).

Simulation

Input parameters for calculating energy use

Honeybee and Ladybug plugins were used for running the energy simulations (Roudsari & Pak, 2013). These plugins were installed on Rhinoceros software (Vantyghem, Ooms, & De Corte, 2021). All geometries were connected to the material by a specific component in the EnergyPlus (US Department of Energy, 2018). This research estimated the total yearly energy loads by the sum of heating and cooling of the building by its gross floor area, which was 50m^2. In this way, the comparison could be made quickly based on every square meter of each zone kWh/m^2. The simulation workflow is shown in Table 4. Based on Table 4, after transferring the single masses to honeybee zones, the zone was set to be conditioned and the program of all zones set to be Midrise Apartment. After setting the Energy Plus (EP construction), EP load and EP schedule, the Heating, Ventilating and Air Conditioning (HVAC) system was imported (Roudsari & Pak, 2013). After running the simulation process, the annual results with the hourly time step were saved based on the kWh/m^2.

Table 3. Window construction details for 3B climate zone.

Type of WID	WID1	WID2	WID3	WID4
U-Value (W/m^2 K)	1.99	2.78	3.41	3.86

Figure 2. Courtyard house as a case study located in Tehran, Iran.

Defining the thermal comfort index (PMV)

Fanger (Fanger, 1972) proposed the Predicted Mean Vote (PMV) model and predicted the occupants' thermal comfort. ISO 07730 (ISO, 07730, 2005) and ASHRAE 55–2013 (ASHRAE, 2013) adopted the PMV model. Most people feel comfortable when the temperature range is 18–30°C, and the humidity

Table 4. Simulation process of this study.

Algorithm 1: Simulation Workflow	
Starting function 1 for all 4 zones	9: Set EP construction (connected all that WLC and WID to the wall and window material)
1: Transform masses to HB zones	10: Set EP loads
2: Zones ← define (the multi zones around the yard by name) Zone1, zone2.zone3, zone4	11: Set EP schedule
3: Set the zones are conditioned or not (they are conditioned)	12: Set HVAC System (ideal air load system)
4: Set the program of all zones (Midrise Apartment)	13-a: cooling set point- 21
5: set WWR for all 4 zones	13-b: heating set point-24
6: X ← defining other variables (design variables)	14: Generate EP output
WLCs-WIDs-	15: Run EP simulation engine
6.1: Set the EP construction for the walls	16: Read the required simulation annual results with the hourly time step
6.2: Set the EP construction for windows	17: Read the thermal load as the first object for the whole year
7: Importing the EP simulation engine	
8: Importing the EPW file6: Set the zones programs (Midrise apartment): Solve the surfaces adjacency	

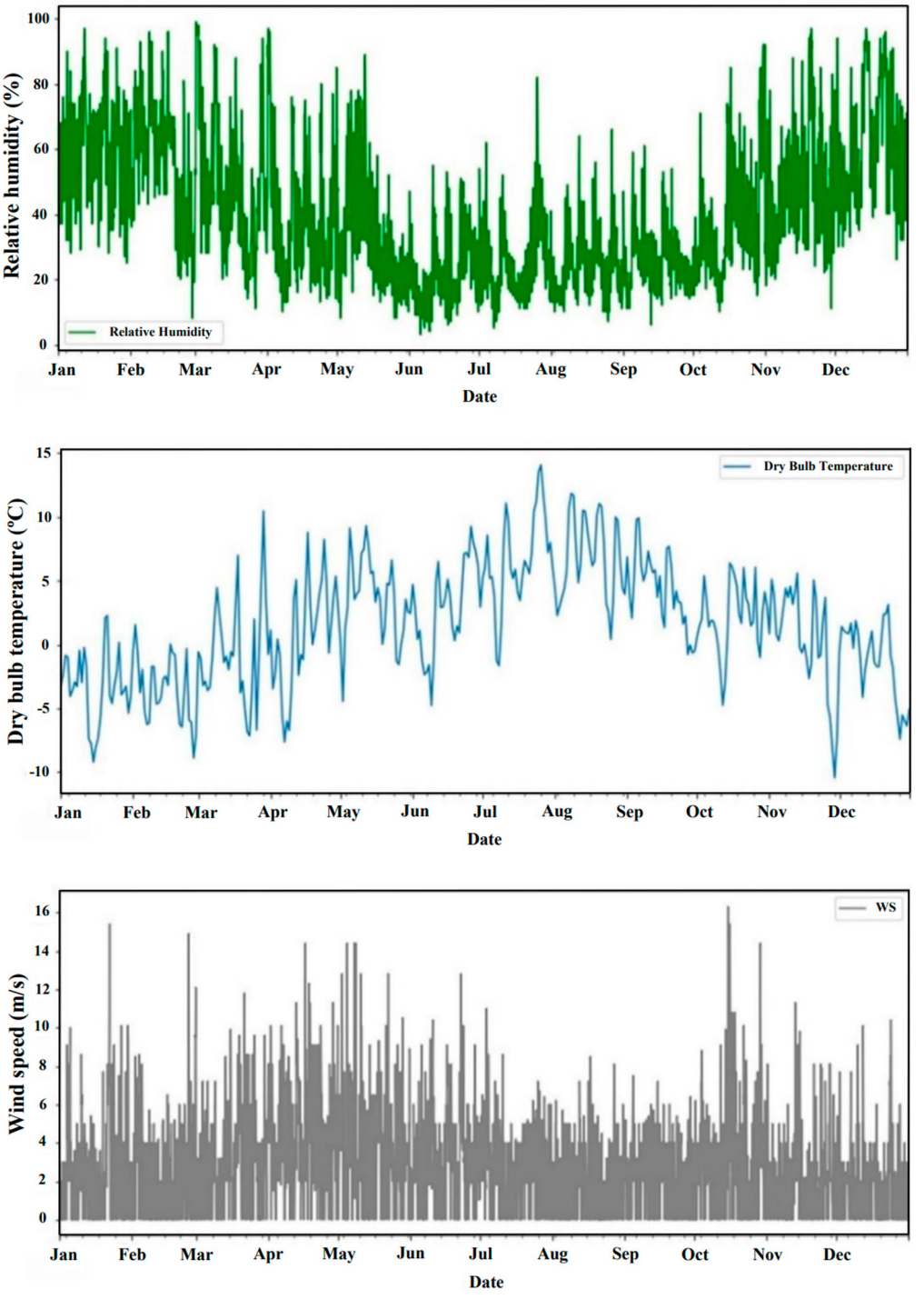

Figure 3. Monthly relative humidity, dry bulb temperature and wind speed based on the EnergyPlus Weather Format (EPW) file of Mehrabad international airport.

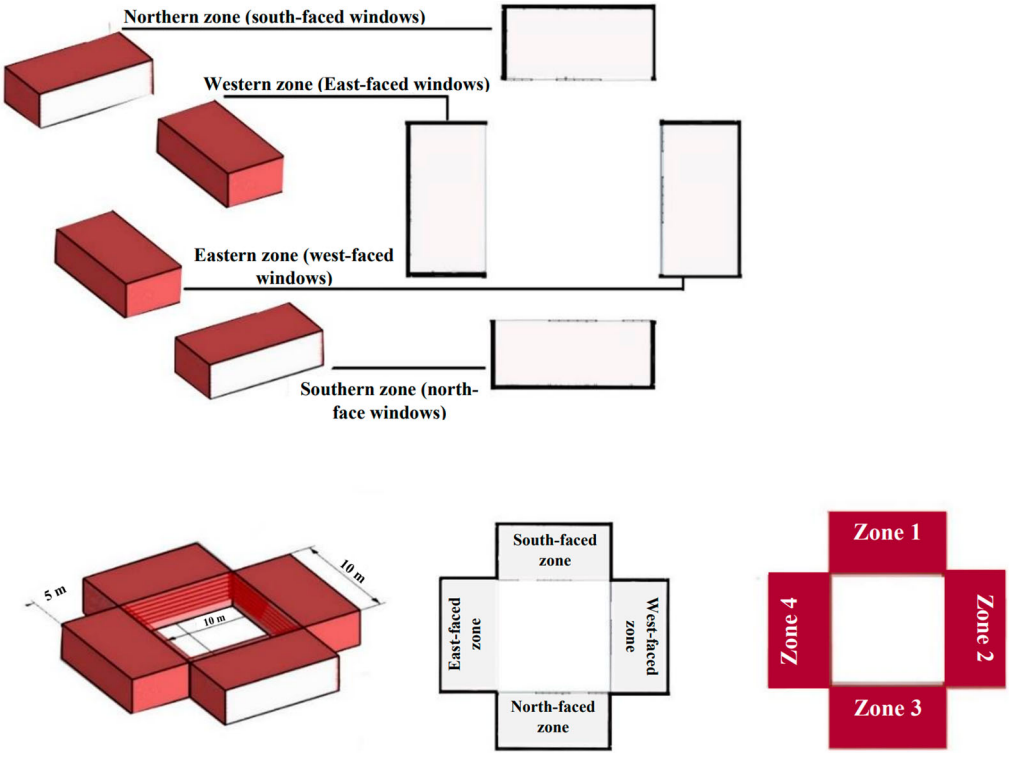

Figure 4. Simulated and real models.

range is 30–70% (Aqilah, Rijal, & Zaki, 2022; Chandel & Sarkar, 2015; Zaki, Damiati, Rijal, Hagishima, & Abd Razak, 2017). PMV is a seven-point scale from cold (−3) to hot (+3) that was used in comfort surveys of P.O. Fanger (Fanger, 1972). Each number shows the following: −3: Cold, −2: Cool, −1: Slightly Cool, 0:Neutral, + 1:Slightly Warm, + 2:Warm, + 3:Hot. Many research used the PMV index to calculate indoor thermal comfort (Pourshaghaghy & Omidvari, 2012; Wu et al., 2019).

After running an energy simulation using Tehran's EPW file, new environmental parameters were achieved for each zone, including relative humidity, air temperature, MRT, and wind speed. These environmental parameters were calculated after simulation in each zone based on different design solutions of each zone, leading to different thermal comfort in each zone.

Calculating PMV value (%) by the PMV comfort component in Ladybug

Regarding the PMV calculation, the PMV comfort component was used in Ladybug tools (Roudsari & Pak, 2013). The optional comfort parameter input could calculate the PMV value for 80% or 90% of people in a comfortable condition. By this option, the whole 8760 h of the year were labeled with a significant point between −3 and 3. If the comfort condition for 90% of the occupant was considered, the whole points between −0.5 to 0.5 were summed together, and the percentage of PMV comfort was calculated around the year. However, when the comfort condition for 80% of the occupant was considered, the points between −1 to –1 were considered to calculate the percentage of comfort level.

In this study, for calculating PMV comfort, the comfort condition for 90% of people was considered. Therefore, all the PMV between −0.5 to –0.5 among the 8760 h were summed and calculated as the year's thermal comfort percentage. It is worth mentioning that in calculating the PMV value, the wind speed was assumed to be very low (0.05 m/s) as suggested by researchers (Leng, Wang, & Liu, 2020). Also, the metabolic rate was considered for a seated human, and the clothing

level was dynamic according to the outdoor air temperature as considered by other researchers (Taylor, Brown, & Rim, 2021). (Table 5)

Parametric study process

The Colibri plugin was used in previous studies (Ibrahim, 2021; Najafi & Pilechiha, 2021; Valitabar, GhaffarianHoseini, GhaffarianHoseini, & Attia, 2022) to perform a parametric analysis to define the objectives for each design solution based on Table 6. The workflow at Colibri divides into two stages: iteration and aggregation. Each level of Colibri contains an Iterator and an Aggregator component. Its operation is comparable to that of the Galapagos (Ilbeigi, Ghomeishi, & Dehghanbanadaki, 2020), a single object optimization engine, while Galapagos is active, the iterator component runs across linked variables and drives the Grasshopper data (Grasshopper, 2021). The WWR, U-value of WID and WLC, DSH, and NSH were inputs for the Colibri plugin, and the objectives were each zone's PMV value and thermal load.

Results

Based on the parametric study results, the BS and WS for all zones were determined, and then, the effect of design parameters (independent variables) on PMV value and thermal load (dependent variables) was assessed. In the next step, the sensitivity analysis was conducted to assess the effect of all independent variables on the PMV value of each zone using SRC. After that, some scatterplots were presented to show the relationship between each zone's most influential variables, PMV values, and thermal loads.

Determination of BS and WS

Based on the simulation results, almost 1000 data were calculated for each zone. The design explorer was used to show the effect of all design solutions simultaneously on objectives (dependent variables). Figures 5–8 show the results in which BS and WS are depicted by green and black lines, respectively. Other lines are possible design solutions.

Zones 1 and 2

Figure 5 and Table 7 show the BS with the most PMV value (94.13%) and least thermal load (184 kWh/m^2/yr) could be calculated for zone 1 when WLC1 and the WID1 with the least U-value of 0.6 W/m^2 K and 1.99 W/m^2 K were considered, respectively. In this case, DSH, NSH, and WWR were the least 0.3 m, 4, and 50%, respectively. Conversely, the least PMV value (86.09%) and the most thermal load of 230 kWh/m^2/yr were achieved for the WS including the WLC4 and WID4 with the highest U-value of 0.93 W/m^2 K and 3.86 W/m^2 K. In this case, the highest NSH (6), DSH

Table 5. Calculation the PMV comfort in Ladybug plugin.

Algorithm 2: calculation the PMV comfort
Starting function 2 (Calculating the PMV comfort)
1: Read the required simulation annual results with the hourly time step from the function 1
2: Extracting the (environmental parameters simulation annual results)
2-a: Air temperature
2-b: Mean radiant temperature
2-c: Relative humidity
3: Connecting the environmental parameters defined above to the PMV comfort calculator component
4: Defining the Metabolic Rate (defined for seated person)
5: Defining the Clothing Level (dynamic based on the outdoor temperature) (Taylor et al., 2021).
6: Run the PMV comfort calculator
7: Read the PMV % as the second objective

Table 6. The process of parametric study by Colibri.

Algorithm 3: Running the parametric study by Colibri
1-Using the Iterator component for collecting all design variables: a-WWR b-WLCs c-WIDs d-NSH e-DSH 2-Using the parameters component for collecting the objectives including a-Thermal load b-PMV (%) 3-Using Aggregator component to collect all data including the design variables and the objectives to set an Excel file to show the result of each design solution a-Genome: The genome in this component is responsible for collecting the design variables. b- Phenome: The phenome in this component is responsible for collecting the objectives. 4- Fly to run the Colibri

(0.5 m), and WWR (70%) were assumed. Therefore, increasing NSH, DSH, and WWR caused to decrease in PMV value and subsequently increase the needed energy to provide thermal comfort for zone 1.

According to Figure 6 and Table 7, the BS with the most PMV value (91.58%) and least thermal load (203 kWh/m^2/yr) were obtained for zone 2 with WLC 2 (with the second least U-value) and WID 1 where the DSH and NSH were the most (0.5 m, 6) and WWR was the least (50%). On the other hand, the least PMV value (82.05%) and the most thermal load of 278 kWh/m^2/yr. were attained for WLC2 and WID3. Also, to calculate the least PMV value, the lowest NSH (4) and DSH (0.3 m), and the highest WWR (70%) were considered. It can be stated that decreasing WWR led to an increase in PMV value for zone 2 similar to what was observed for zone 1. However, contrary to zone 1, increasing NSH and DSH for zone 2 contributed to achieving the BS, the most cost-effective way to provide thermal comfort.

Zones 3 and 4

According to Figures 7 and 8 and Table 8, similar results were attained for zones 3 and 4, where the greatest PMV values (93.71% and 92.23%) and the least thermal loads (190 and 197 kWh/m^2/yr.) were obtained once the lowest WWR (50%) and the highest DSH (0.5 m) and NSH (6) were considered. In this case, WLC 1 with the least U-value of 0.6W/m^2 K, and WID 1 with the least U-value of 1.99 W/m^2 K were used. On the other hand, the highest WWR (70%) and the lowest DSH (0.3 m) and NSH (4) resulted in the WS in which the WLC4 and WID4 with the highest U-value of 0.93 and 3.86 W/m^2 K were employed.

According to Tables 7 and 8, the lowest WWR for all zones contributed to the highest PMV values with the lowest thermal loads. In addition to this, similar to the results of zone 2, increasing DSH and NSH for zones 3 and 4 led to the greatest PMV values with the highest thermal comfort, while the reverse was observed for zone 1.

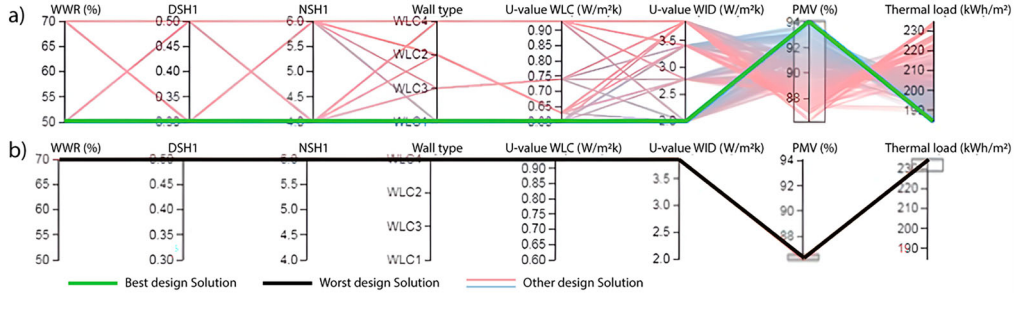

Figure 5. BS (A) and WS (B) for zone 1.

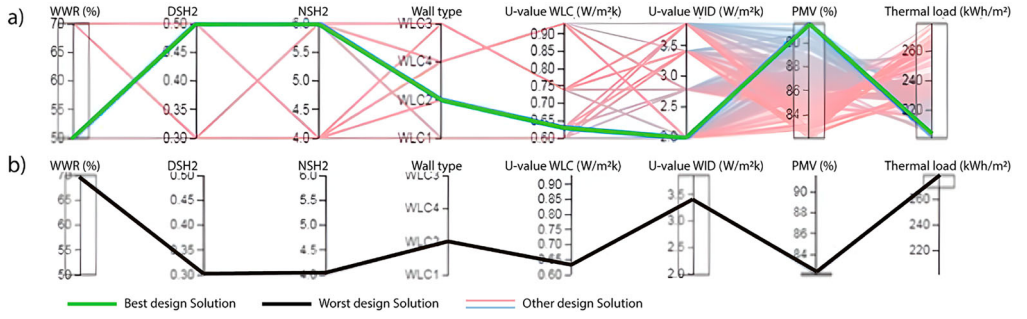

Figure 6. BS (A) and WS (B) for zone 2.

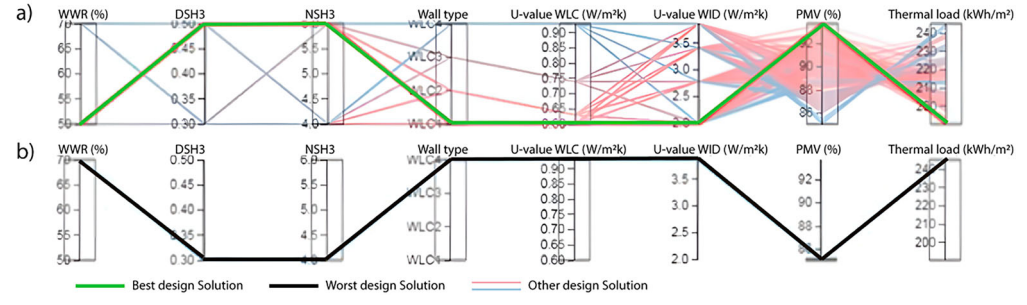

Figure 7. BS (A) and WS (B) for zone 3.

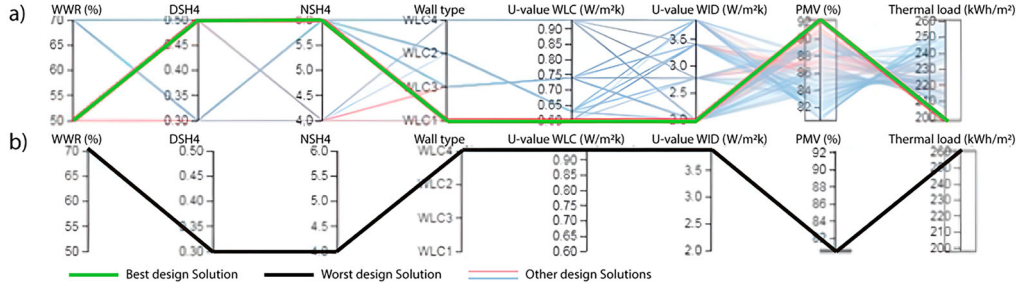

Figure 8. BS (A) and WS (B) for zone 4.

Independent variables' effects on PMV value and thermal load

Effect of WWR

As shown in Figure 9(a–h), the WWR of 70% contributed to the highest thermal load and least thermal comfort for all four zones when the WLC4 with the highest U-value was selected. However, in all cases, the WWR of 50% associated with the WLC1 with the least U-value led to the least thermal load and highest thermal comfort. Considering all WLC, the WWR of all zones had a distinct influence on the thermal load, meaning that the WWRs of 70% and 50% resulted in the highest and lowest energy consumption, respectively.

Effect of DSH

As shown in Figure 10(a–h), the least thermal load and highest thermal comfort were for zone 1 (south-faced zone) when the WLC 1 was used and the depth of shading was 0.3 m. However, the

Table 7. Comparison of PMV value and thermal load for real case, best design solution, and worst design solution in zones 1 and 2.

		Zone 1			Zone 2		
Type of variables	Variables	Best solution	Worst solution	Real case	Best solution	Worst solution	Real case
Independent	V1-1-WWR of zone 1 (%)	50	70	70	–	–	–
	V1-1-WWR of zone 2 (%)	–	–	–	50	70	70
	V5-DSH (m)	0.3	0.5	0.3	0.5	0.3	0.3
	V6-NSH	4	6	4	6	4	4
	V7-Walltype	WLC1	WLC4	WLC4	WLC2	WLC4	WLC4
	V8: WID	WID1	WID4	WID4	WID1	WID3	WID4
Dependent	PMV value (%)	94.13	86.09	88.51	91.58	82.05	85.6
	Thermal load (kWh/m^2/yr.)	184	234	220	203	278	245

Table 8. Comparison of PMV value and thermal load for real case, best design solution, and worst design solution in zones 3 and 4.

		Zone 3			Zone 4		
Type of variables	Variables	Best solution	Worst solution	Real case	Best solution	Worst solution	Real case
Independent	V1-3-WWR of zone 3 (%)	50	70	70	–	–	–
	V1-4-WWR of zone4 (%)	–	–	–	50	70	70
	V5-DSH (m)	0.5	0.3	0.3	0.5	0.3	0.3
	V6-NSH	6	4	4	6	4	4
	V7-Walltype	WLC1	WLC4	WLC4	WLC1	WLC4	WLC4
	V8: WID	WID1	WID3	WID4	WID1	WID4	WID4
Dependent	PMV value (%)	93.71	85.05	88.12	92.23	80.60	83.45
	Thermal load (kWh/m^2/yr.)	190	245	224	197	260	238

least thermal comfort and highest thermal load of zone 1 were for the WLC 4 with a DSH of 0.5 m. Concerning zone 2 to zone 4, the least energy consumption and highest PMV value were for the most increased depth of shading, 0.5 m, but the highest thermal load and the least thermal comfort were yielded when the WLC4 was used and the least depth of shading was 0.3 m, having an influential role based on the location of the zones.

Effect of NSH

According to Figure 11(a–h), the least thermal load and highest thermal comfort were for zone1 when the WLC 1 was used and the number of shading was 4, demonstrating that zone 1 with the southern window should have less shading to show the best performance in this multiple zone house. In zones 2, 3, and 4, the highest thermal comfort and the least thermal load were achieved when the WLC 1 was used and the number of shading was 6. Considering the least number of shading (4) led to the best energy performance for zone 1, while fewer PMV values and high thermal loads were obtained for other zones. Moreover, the highest thermal load and the least thermal comfort were for zone 2 to zone 4 when the WLC4 was used and the number of shading was 4 (the least number of shading).

Effect of WID

Based on Figure 12(a–h), in zones 1,3, and 4, the least thermal load and highest thermal comfort could be achieved when the WLC 1 with the lowest U-value and the WID 1 with the least U-value

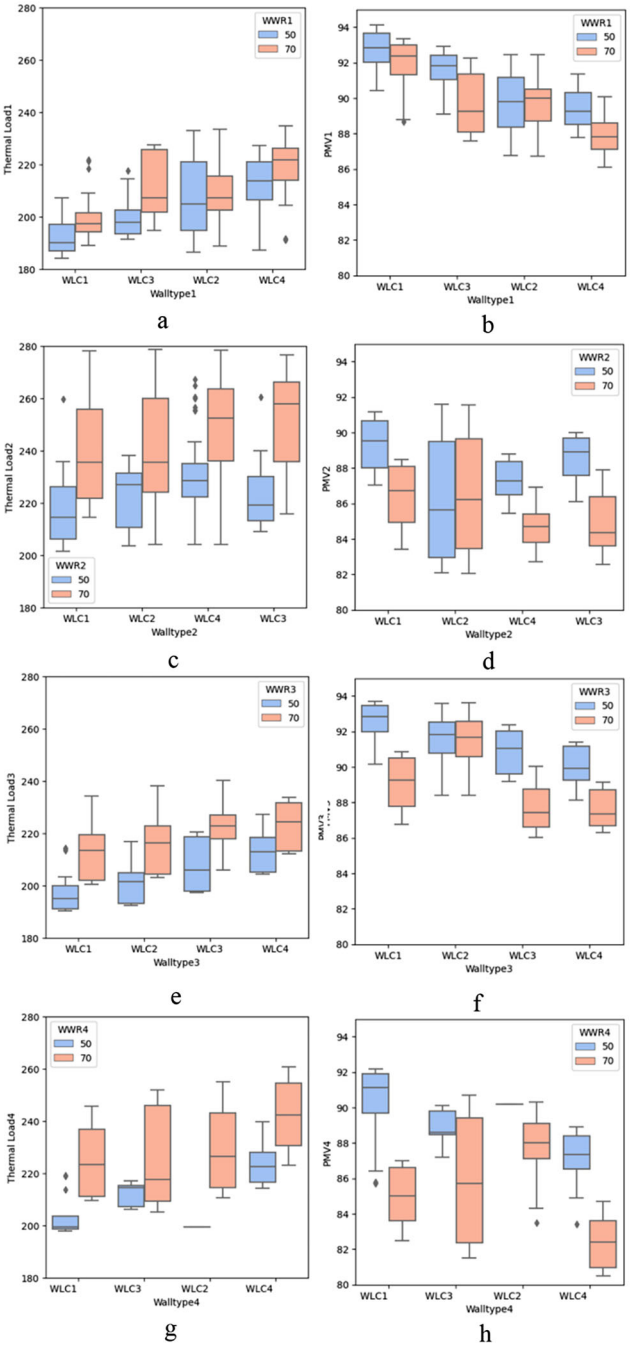

Figure 9. The relationship of the Wall type and WWR with thermal comfort and thermal load.

was chosen. Moreover, when other wall types were considered for zones 1, 3, and 4, the highest thermal load and least thermal comfort were attained for WID4 with the highest U-value. In addition, in zone 2, the highest thermal load and least thermal comfort were for the WLC3 and WID3 with the second highest U-value.

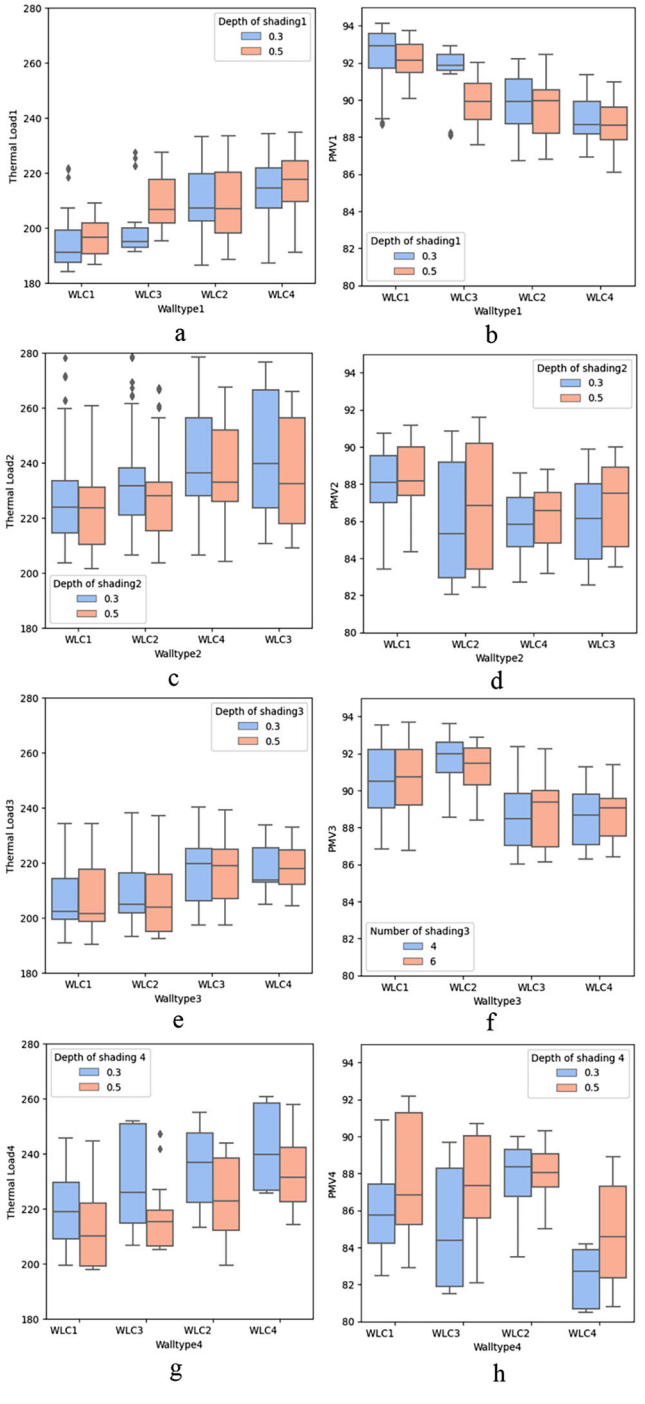

Figure 10. The relationship of the Wall type and DSH with dependent variables.

The comparison of PMV value and thermal load for RC, BS, and WS

As per Figure 13, the comparison of WS and BS showed that the PMV value of zone 1 increased by about 8%, and the thermal load decreased by 21%. Moreover, there was a thermal load reduction of

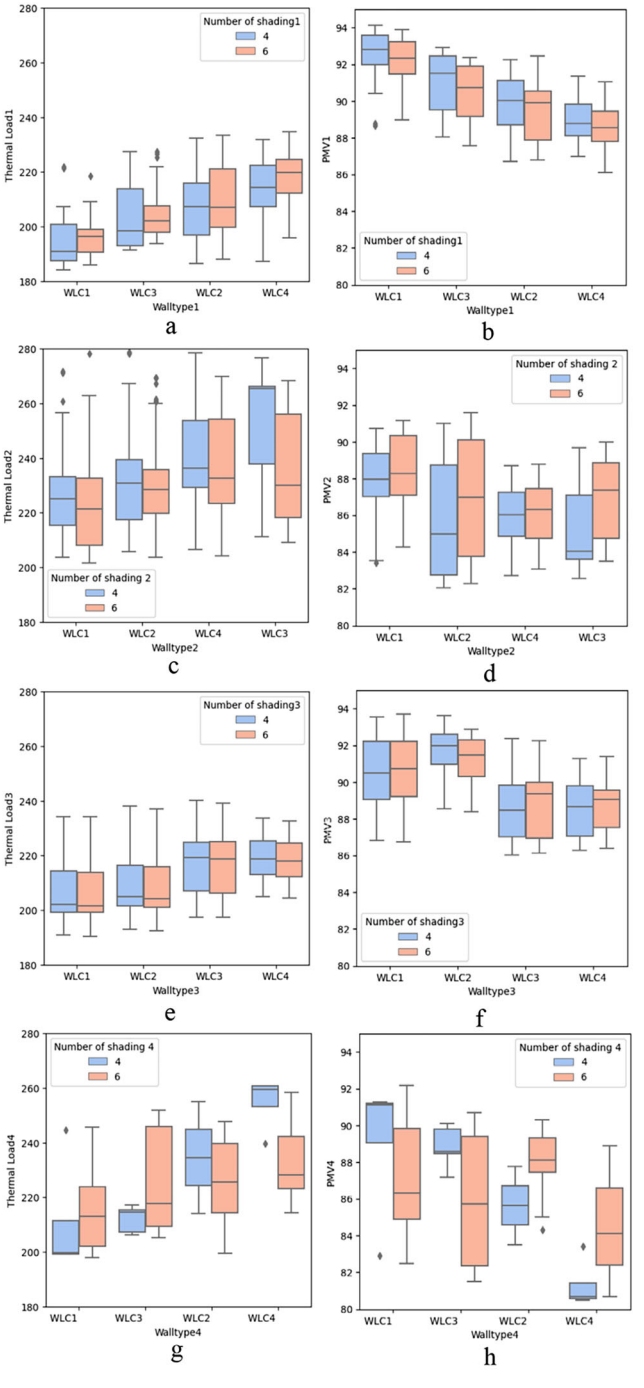

Figure 11. The relationship of the Wall type and NSH with dependent variables.

around 16% in BS compared to the RC, and there was more thermal comfort in BS than in the RC. Comparing WS and BS, it was observed that the PMV value of zone 2 increased by about 9%, and the thermal load decreased by about 26%.

Furthermore, there was a reduction of thermal load of around 16% in BS compared to the RC, and there was 6% more thermal comfort in BS than in the RC. In zone 3, the PMV of BS increased by 8%

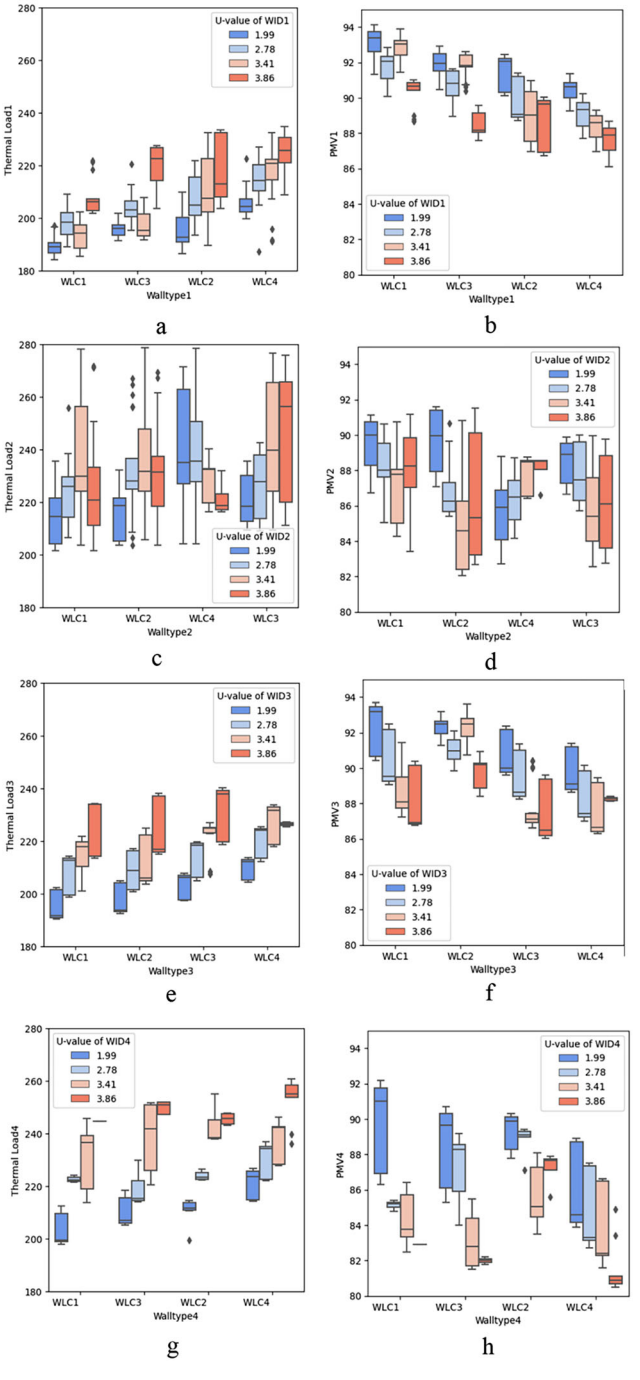

Figure 12. The relationship of the Wall type and WID with dependent variables.

compared to the WS and 6% compared to the RC. Also, there was a reduction of 22% in the thermal load of BS compared to the WS and 15% compared to the RC.

Finally, in zone 4, the PMV of BS increased by 12% more than the PMV of WS, and the thermal load decreased by around 21%. The comparison of BS and RC of zone 4 presented an increase of 9% and a

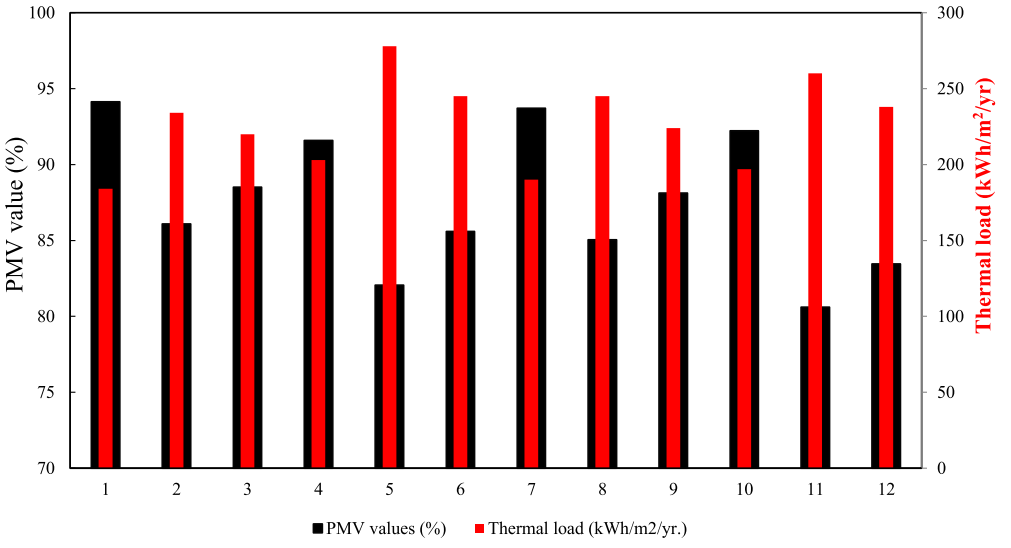

Figure 13. The PMV value and thermal comparison for RC, BS, and WS.

reduction of 17% for the PMV value and thermal load, respectively. The most reduction of energy consumption was for zone 2, and the most improvement in thermal comfort was for zone 4.

Sensitivity analysis

SRC analysis of design parameters

Since there was a limited design variable in this research, SCR before running the parametric study was not considered. However, it is recommended to be sure about the most influential variable and its effect on both PMV values. In other words, the effect of the strongest variable in each zone could be examined by the SRC. R software was used in this section to calculate the effect of design parameters (independent variables) on the objectives (dependent variables). As for building energy analysis, the Regression technique was used among many methods (Tian, 2013). The indicator used for the sensitivity analysis of this study was SRC, as suggested by other researchers (Yang, 2013).

SRC analysis for each zone

A larger absolute value of SRC showed a larger impact of design parameters on objectives. Design options were earned in the simulation process for each zone used for the sensitivity analysis to illustrate the effect of each independent variable on the objectives. Based on Figure 14, the SRC analysis for each zone is listed as follows:

- In zone 1, the most influential variable with a negative impact on PMV value was WID, WLC, and WWR, about −.44, −0.35, and −0.22, respectively, contributing to decreasing the PMV value. The effect of DSH and NSH was negligible.
- For the PMV value of zone 2, the most influential variable was the WWR (−0.43), decreasing the PMV value. The second most negative effect was for WLC (−0.28). The effect of DSH and NSH were positive at 0.14 and 0.1.
- In zone 3, the most influential variable with a negative impact on PMV value was WID, WWR, and WLC, about −.51, −0.46, and −0.45, respectively, contributing to decreasing the PMV value. The effect of DSH and NSH was negligible.

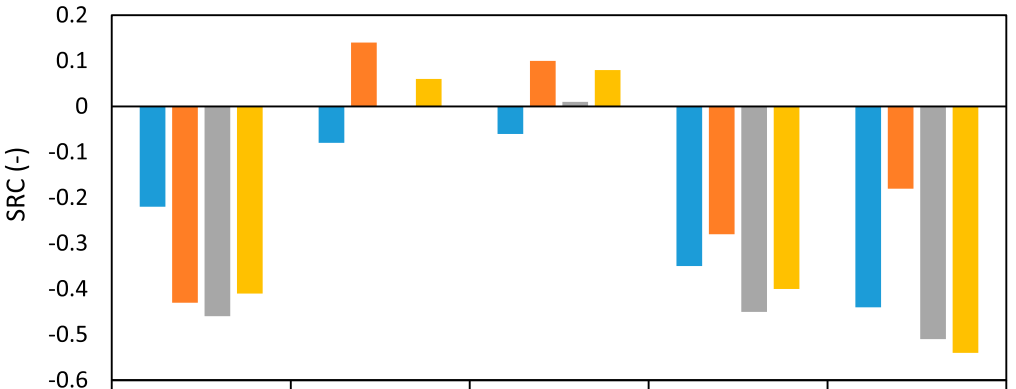

	WWR	DSH	NSH	WLC	WID
Zone 1	-0.22	-0.08	-0.06	-0.35	-0.44
Zone 2	-0.43	0.14	0.1	-0.28	-0.18
Zone 3	-0.46	0	0.01	-0.45	-0.51
Zone 4	-0.41	0.06	0.08	-0.4	-0.54

Figure 14. The effect of variables on the PMV value (sensitivity of regression coefficient)

- The most influential variable on the PMV value of zone 4 was WID (−0.54). The WWR (−0.41) and WLC (−0.40) followed this trend. The effect of DSH and NSH was negligible.
- The PMV comfort of the only zone most negatively affected by WID and WWR was zone 4 and zone 3, respectively.

Scatterplots of PMV values and variables

The result was collected through around 1000 simulations for each zone in scatterplots. Each data point represented one design option. The scatterplots based on Figures 15–17 were developed to show the correlations of each zone's PMV value, thermal load, and the most effective mentioned variables.

The most effective variables on PMV values

Based on the sensitivity analysis mentioned in section 3.4.2, the effect of WID on the PMV value of zones 1, 3, and 4 was measured. Figure 14 presents that the SRC of WID of zones 1, 2, and 3 were −0.44, −0.51, and −0.54, respectively. Then, some scatterplots based on Figures 15–17 were developed to show the relationship of the WID with PMV value and the thermal load of each zone.

Figure 15 presents that in zones 1, 3 and 4, the WID with the higher U-value around 3.86 W/m^2 K led to less PMV value, whereas the U- value of 1.99 W/m^2 K resulted in higher PMV values.

The second most influential variable in zones 1 and 2 was the WLC, about −0.35 and −0.28. Based on Figure 16, the WLC with a U-value of 06-0.63 W/m^2 K contributed to the higher PMV value, and the WLC with a U-value of 0.74-0.93 W/m^2 K led to decreasing PMV value and increasing thermal load.

The most influential variable in zone 2 and the second highest in zones 3 and 4 were WWR, around −0.43, −0.46, and −0.41. Based on Figure 17, in three zones, as a general truth, the WWR of 50% contributed to the higher PMV, while the WWR of 70% caused less PMV comfort and more thermal load.

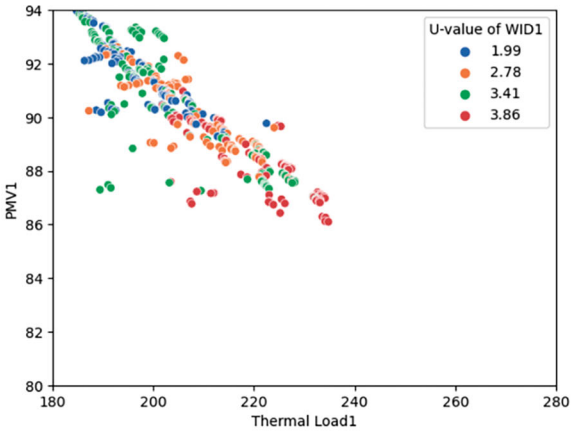

a

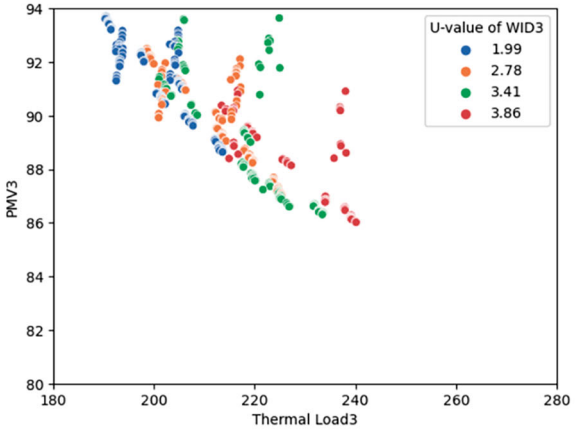

b

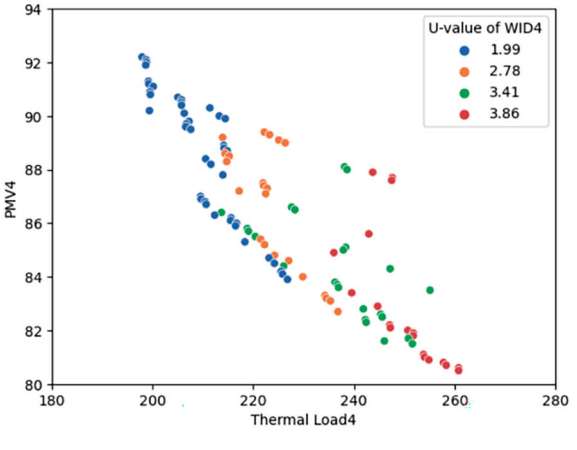

c

Figure 15. Comparison of PMV vs. thermal load by U-value of window construction in zones 1, 3, and 4.

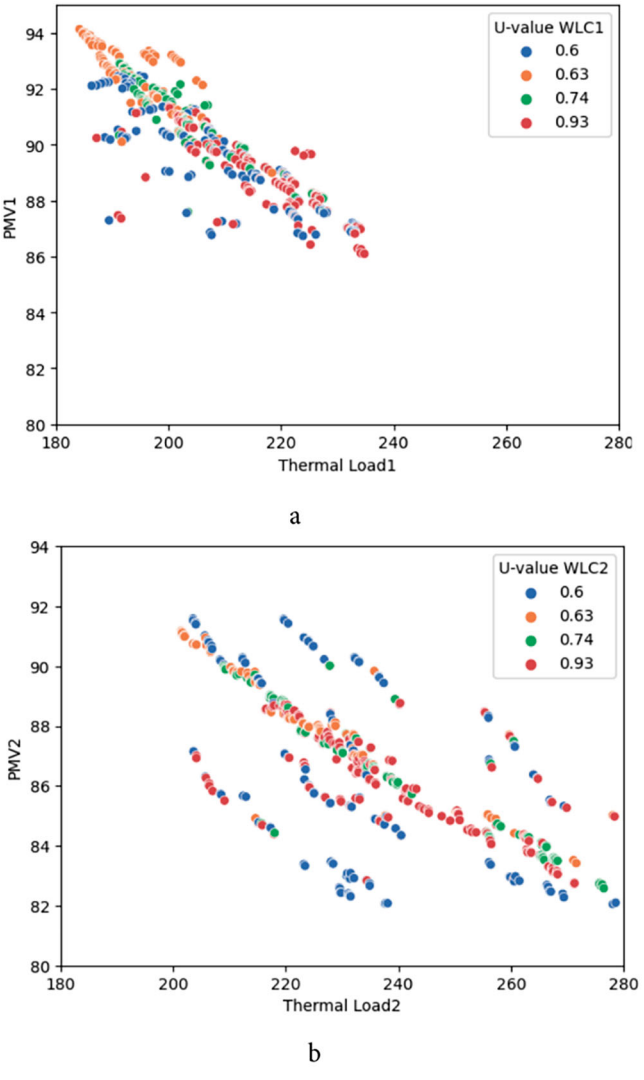

Figure 16. Comparison of PMV vs. thermal load by U-value of wall construction in zones 1 and zone 4.

Discussion

Based on the SRC, the effect of WID with different U-value in zones1, 3 and 4 was more critical than the WLC on PMV value. However, WLC was more influential than WID in zone 2. The reason is that zone 2 with the western window received less solar radiation during the day. Therefore, the effect of WLC on the energy performance of zone 2 was more than that of WID, while the reverse was observed for other zones. Also, Kalogirou et al. (Kalogirou et al., 2002) demonstrated that the energy saving of building was highly dependent on the thermal performance of WID. Soflaei et al. (Soflaei et al., 2020) stated that the effect of WLC on the thermal comfort of courtyard houses was more important than the effect of WID in the courtyard design of BWh climate. Therefore, the results were not comparable with the results of this study. The most important reason for this is the climate, WWR, glazing type, and the zones' location. Regarding this, a sensitivity analysis by Samuelson et al. (Samuelson, Claussnitzer, Goyal, Chen, & Romo-Castillo, 2016) revealed that WWR was the most sensitive variable, followed by building rotation and glass type. Similarly, Hinkle

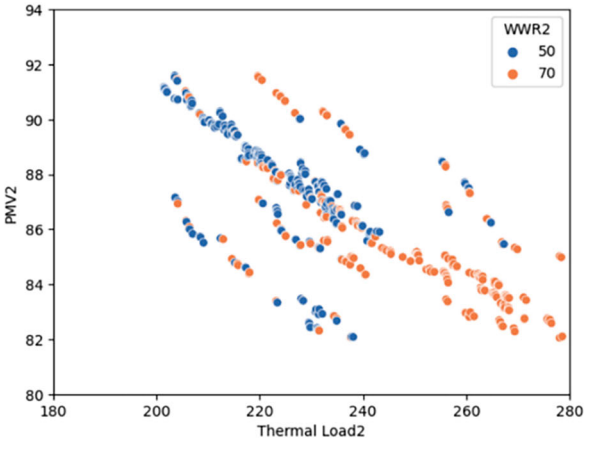

a

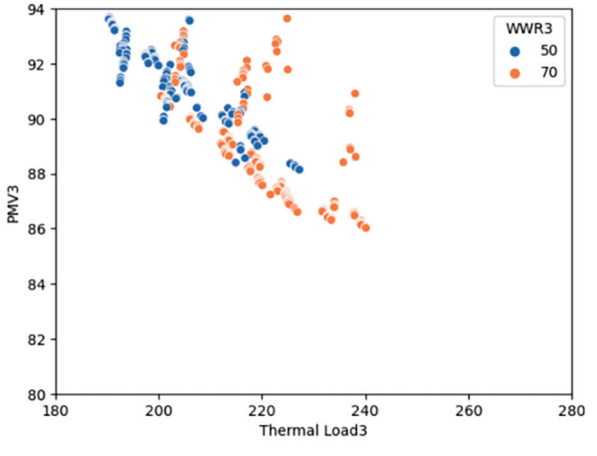

b

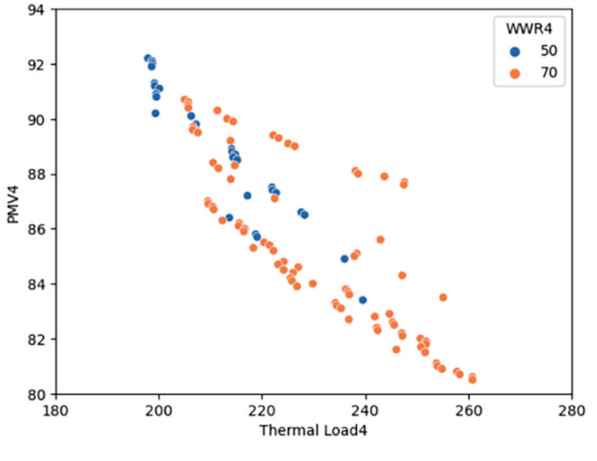

c

Figure 17. Comparison of PMV vs. thermal load by WWR in zones 2, 3 and 4.

et al. (Hinkle et al., 2022) showed that WWR and window performance were the two parameters that were most crucial for predicting building energy usage. In this study, the materials used in WLC differed from those stated by Soflaei et al. (Soflaei et al., 2020). Furthermore, the WID used in the current research was based on the 3B ASHRAE climate zone, completely different from the glazing type stated in the research above. The BWh climate of different states in the USA was not comparable with this research work's 3B climate zone. The location of the zones was another reason for the difference between the results of this study and those given by Soflaei et al. (Soflaei et al., 2020). Therefore, different design solutions contributed to the different thermal comfort values, including the WWR, U-value of WLC and WID, the window position, and the zone location.

It is clear that different material characteristics, including opaque and transparent material with different U-values led to different thermal comfort (Kazemi, Rahif, Courard, & Attia, 2023; Kazemi & Courard, 2021b). For example, in this specific research, the less U-value of WLC contributed to less thermal load. However, in this study, when the U-value was less in winter, fewer heat was transferred to the outside of the building and consequently less energy was wasted. A similar result was given by de Rubeis et al. (de Rubeis et al., 2018). According to this study, the performance of materials in the winter season in Italy was evaluated. The authors concluded that low U-value material decreased heat loss. In the same line, the finding showed that the four wall materials used in the current research illustrated different thermal performances and obtained different thermal comfort ranges. According to the results, WLC with the highest U-value had a negative effect on thermal load and PMV value in all zones of the courtyard house. Wall types 1 and 2 obtained higher thermal comfort levels than wall types 3 and 4 due to the low U-values. Fernandes et al. (Fernandes et al., 2019) showed that in a climate condition such as Istanbul, higher U-values led to more significant energy consumption in heavyweight construction than in lightweight construction. It was consistent with our research showing that the high thermal mass with a high U-value, like the WLC4 with the core 4, had a negative effect on energy consumption in Tehran's hot and arid climate. Based on the result, the core 4 with a higher U-value was a less favorable core structure than cores 1 and 2. Moreover, this was consistent with de Rubies et al. (de Rubeis et al., 2018) who studied the thermal performance of materials in the winter season in Italy. The authors concluded that material with a low U-value decreased heat loss. Similarly, the findings of current research showed that the wall construction with the cores 1 and 2 with less U-value around 0.6-0.67 (W/m^2K) compared to other cores showed a better performance in increasing PMV value and decreasing the energy consumption in different zones.

As for the location of the zone and the window position in the courtyard house, our research showed that zone 1 located in the north with a southern window, had a better performance in terms of thermal comfort and thermal load; however, zone 2 with western window contributed to the least PMV value. The simulation studies achieved a similar result by Pilechiha et al. (Pilechiha et al., 2021). They proved that the northern zone with southern windows had more thermal comfort in the winter, around six times more than the south zone with north windows. This was because of absorbing direct radiation in winter and not receiving the irritating radiation in summer.

Conclusions

This study analyzed the effect of design parameters on the predicted mean vote value and thermal load under the climate of cold and semi-arid Tehran. Based on the results, following conclusions can be drawn:

- Among the four zones around the courtyard, zone1 (northern zone with the southern window) had the most thermal comfort and least thermal load in the optimized solution. The second highest thermal comfort and least energy consumption were for zone 3 (southern zone with northern window). This was followed by zone 4 (western zone), and zone 2 (eastern zone).

- The maximum thermal comfort of zone 1 (94.13%) was obtained for a zone with the WLC1, WID1, with the least U-value, and the least window to wall ratio (50%), depth of shading (0.3 m) and number of shading (4).
- The maximum thermal comfort of zone 2–4, about 91.58%, 93.71%, 92.23%, respectively, was obtained for a zone with the WLC1, WID1, with the least U-value, and the least window to wall ratio (50%), and with the most depth of shading (0.5) and number of shading (6).
- For zones 1, 3, and 4, WLC1 and WLC2 were recognized as the best and worst wall construction, respectively. Moreover, the WLC2 had the second least U-value among the four wall constructions (0.63 W/m^2 K) and for zone 2, it was calculated as the best and worst construction, meaning that zone 2 should consider another variable to maximize the thermal comfort, such as window to wall ratio.
- According to the results of the standard regression coefficient, almost all parameters caused quite significant effects on the predicted mean vote value. For this reason, while designing a multi-zone house, the window construction and many parameters such as wall construction, window to wall ratio, and the shading characteristics should be considered simultaneously.
- The predicted mean vote values of all zones was negatively affected by window construction, wall construction, and window to wall ratio. In addition, the predicted mean vote values of all zones except for zone2 were most negatively affected by window construction.
- In zones 2, 3, and 4, window to wall ratio was considered one of the influential variables, but the window to wall ratio of zone 1 was not as significant as that of other zones.
- The effect of the shading characteristics was negligible in zones 1 and 3. Also, the effect of depth of shading and the number of shading in zone 2 with the western window were more significant than that in other zones.

In brief, it was vital to carefully analyze the design parameters before the construction to increase the predicted mean vote values and reduce the thermal loads in all seasonal zones of the courtyard. For future investigation, the first recommendation is to analyze material on thermal comfort in different climate zones. Also, instead of the predicted mean vote comfort, the indoor adaptive thermal comfort can be estimated for an entirely passive house design.

Disclosure statement

No potential conflict of interest was reported by the author(s).

References

Alkalbani, S., Rezgui, Y., Vorakulpipat, C., & Wilson, I. E. (2013). ICT adoption and diffusion in the construction industry of a developing economy: The case of the sultanate of Oman. *Architectural Engineering and Design Management*, *9*(1), 62–75. doi:10.1080/17452007.2012.718861

Al-Saadi, S. N. (2006). *Envelope design for thermal comfort and reduced energy consumption in residential buildings*. https://scholar.google.com/scholar_lookup?title=Envelope%20design%20for%20thermal%20comfort%20and%20reduced%20energy%20consumption%20in%20residential%20buildings&publication_year=2006&author=S.N.%20Al-Saadi.

ANSI/ASHRAE Standard 90.1. (2019). *Energy standard for buildings except low-rise residential buildings*. American Society of Heating, Refrigerating and Air Conditioning Engineers (Atlanta, Georgia). New York, NY: ASHRAE.

Aqilah, N., Rijal, H. B., & Zaki, S. A. (2022). A review of thermal comfort in residential buildings: Comfort threads and energy saving potential. *Energies*, *15*(23), 9012. doi:10.3390/en15239012

ASHRAE. (2004). *Thermal environmental conditions for human occupancy*. ANSI/ASHRAE Standard 55-2004. doi:10.1007/s11926-011-0203-9

ASHRAE. (2013). *Standard 55-2013—thermal environmental* conditions for human occupancy. Atlanta, GA: ASHRAE.

ASHRAE. (2017). *Handbook of fundamentals*. Atlanta, GA: ASHRAE.

Aydın, D., & Mıhlayanlar, E. (2020). A case study on the impact of building envelope on energy efficiency in high-rise residential buildings. *Architecture, Civil Engineering, Environment (ACEE Journal)*, *13*(1), 5–18.

Bakmohammadi, P., & Noorzai, E. (2020). Optimization of the design of the primary school classrooms in terms of energy and daylight performance considering occupants' thermal and visual comfort. *Energy Reports*, *6*, 1590–1607.

Bhatnagar, S., Jacob, G., Devkar, G., Rybkowski, Z. K., Arefazar, Y., & Obulam, R. (2022). A systematic review of lean simulation games in the construction industry. *Architectural Engineering and Design Management*, *0*(0), 1–19. doi:10.1080/17452007.2022.2155604

Brown, N. C., Jusiega, V., & Mueller, C. T. (2020). Implementing data-driven parametric building design with a flexible toolbox. *Automation in Construction*, *118*, 1–16, 103252. doi:10.1016/j.autcon.2020.103252

Carlucci, S., Bai, L., de Dear, R., & Yang, L. (2018). Review of adaptive thermal comfort models in built environmental regulatory documents. *Building and Environment*, *137*, 73–89. doi:10.1016/j.buildenv.2018.03.053

Carmody, J., Selkowitz, S., Lee, E. S., Arasteh, D., & Willmert, T. (2004). *Window system for high-performance buildings*. https://scholar.google.com/scholar_lookup?title=Window%20systems%20for%20high-performance%20buildings&publication_year=2004&author=J.%20Carmody

Chandel, S. S., & Sarkar, A. (2015). Performance assessment of a passive solar building for thermal comfort and energy saving in a hilly terrain of India. *Energy and Buildings*, *86*, 873–885. doi:10.1016/j.enbuild.2014.10.035

Cuce, E., & Riffat, S. B. (2015). Vacuum tube window technology for highly insulating building fabric: An experimental and numerical investigation. *Vacuum*, *111*, 83–91. doi:10.1016/j.vacuum.2014.10.002

De Dear, R., Kim, J., Candido, C., & Deuble, M. (2015). Adaptive thermal comfort in Australian school classrooms. *Building Research & Information*, *43*(3), 383–398. doi:10.1080/09613218.2015.991627

de Rubeis, T., Nardi, I., Ambrosini, D., & Paoletti, D. (2018). Is a self-sufficient building energy efficient? Lesson learned from a case study in Mediterranean climate. *Applied Energy*, *218*, 131–145. doi:10.1016/j.apenergy.2018.02.166

Efeoma, M. O., & Uduku, O. (2014). Assessing thermal comfort and energy efficiency in tropical African offices using the adaptive approach. *Structural Survey*, *32*, 396–412.

Enescu, D. (2017). A review of thermal comfort models and indicators for indoor environments. *Renewable and Sustainable Energy Reviews*, *79*(February), 1353–1379. doi:10.1016/j.rser.2017.05.175

Fanger, P. (1972). Thermal comfort: Analysis and applications in environmental engineering. *Applied Ergonomics*, *3*(3), 181. doi:10.1016/S0003-6870(72)80074-7

Fathy, H. (2014). Natural energy and vernacular architecture. *Natural Energy and Vernacular Architecture*, 28–32.

Fernandes, M. S., Rodrigues, E., Gaspar, A. R., Costa, J. J., & Gomes, Á. (2019). The impact of thermal transmittance variation on building design in the Mediterranean region. *Applied Energy*, *239*, 581–597. doi:10.1016/j.apenergy.2019.01.239

Ghaffour, W., Ouissi, M. N., & Velay Dabat, M. A. (2020). Analysis of urban thermal environments based on the perception and simulation of the microclimate in the historic city of Tlemcen. *Smart and Sustainable Built Environment*, *10*(2), 141–168. doi:10.1108/SASBE-12-2019-0166

Grasshopper. (2021). *Algorithmic modeling for Rhino*. https://www.grasshopper3d.com/

Gregory, K., Moghtaderi, B., Sugo, H., & Page, A. (2008). Effect of thermal mass on the thermal performance of various Australian residential constructions systems. *Energy and Buildings*, *40*(4), 459–465. doi:10.1016/j.enbuild.2007.04.001

Hinkle, L. E., Wang, J., & Brown, N. C. (2022). Quantifying potential dynamic façade energy savings in early design using constrained optimization. *Building and Environment*, *221*, 109265. doi:10.1016/j.buildenv.2022.109265

Ibrahim, Y. (2021). *Dataset for "a parametric optimisation study of urban geometry design to assess outdoor thermal comfort"*.

Ilbeigi, M., Ghomeishi, M., & Dehghanbanadaki, A. (2020). Prediction and optimization of energy consumption in an office building using artificial neural network and a genetic algorithm. *Sustainable Cities and Society*, *61*, 102325. doi:10.1016/j.scs.2020.102325

ISO 07730. (2005). *Ergonomics of the thermal environment – analytical determination and interpretation of thermal comfort using calculation of the PMV and PPD indices and local thermal comfort criteria*.

Jaffal, I., Inard, C., Ghaddar, N., & Ghali, K. (2020). A metamodel for long-term thermal comfort in non-air-conditioned buildings. *Architectural Engineering and Design Management*, *16*(6), 441–472. doi:10.1080/17452007.2020.1719813

Jang, N., & Ham, S. (2017). A study on courtyard apartment types in South Korea from the 1960s to 1970s. *Frontiers of Architectural Research*, *6*(2), 149–156. doi:10.1016/j.foar.2017.03.004

Javed, S., Ørnes, I. R., Myrup, M., & Dokka, T. H. (2019). Design optimization of the borehole system for a plus-Energy kindergarten in Oslo, Norway. *Architectural Engineering and Design Management*, *15*(3), 181–195. doi:10.1080/17452007.2018.1555088

Jelle, B. P., Hynd, A., Gustavsen, A., Arasteh, D., Goudey, H., & Hart, R. (2012). Fenestration of today and tomorrow: A state-of-the-art review and future research opportunities. *Solar Energy Materials and Solar Cells*, *96*, 1–28. doi:10.1016/j.solmat.2011.08.010

Kalogirou, S. A., Florides, G., & Tassou, S. (2002). Energy analysis of buildings employing thermal mass in Cyprus. *Renewable Energy*, *27*(3), 353–368. doi:10.1016/S0960-1481(02)00007-1

Kazemi, M., & Courard, L. (2021a). Modelling hygrothermal conditions of unsaturated substrate and drainage layers for the thermal resistance assessment of green roof: Effect of coarse recycled materials. *Energy and Buildings*, *250*, 111315. doi:10.1016/j.enbuild.2021.111315

Kazemi, M., & Courard, L. (2021b). Simulation of humidity and temperature distribution in green roof with pozzolana as drainage layer: Influence of outdoor seasonal weather conditions and internal ceiling temperature. *Science and Technology for the Built Environment*, *27*(4), 509–523. doi:10.1080/23744731.2021.1873658

Kazemi, M., Courard, L., & Attia, S. (2023). Water permeability, water retention capacity, and thermal resistance of green roof layers made with recycled and artificial aggregates. *Building and Environment*, *227*, 109776. doi:10.1016/j.buildenv.2022.109776

Kazemi, M., Courard, L., & Hubert, J. (2021). Heat transfer measurement within green roof with incinerated municipal solid waste aggregates. *Sustainability*, *13*(13), 7115. doi:10.3390/su13137115

Kazemi, M., Courard, L., & Hubert, J. (2022). Coarse recycled materials for the drainage and substrate layers of green roof system in dry condition: Parametric study and thermal heat transfer. *Journal of Building Engineering*, *45*, 103487. doi:10.1016/j.jobe.2021.103487

Kazemi, M., Rahif, R., Courard, L., & Attia, S. (2023). Sensitivity analysis and weather condition effects on hygrothermal performance of green roof models characterized by recycled and artificial materials. *Building and Environment*, *237*, 1–15.

Kishore, R. A., Bianchi, M. V. A., Booten, C., Vidal, J., & Jackson, R. (2021). Enhancing building energy performance by effectively using phase change material and dynamic insulation in walls. *Applied Energy*, *283*, 116306. doi:10.1016/j.apenergy.2020.116306

Lee, J., Kim, J., Song, D., Kim, J., & Jang, C. (2017). Impact of external insulation and internal thermal density upon energy consumption of buildings in a temperate climate with four distinct seasons. *Renewable and Sustainable Energy Reviews*, *75*, 1081–1088.

Leng, J., Wang, Q., & Liu, K. (2020). Sustainable design of courtyard environment: From the perspectives of airborne diseases control and human health. *Sustainable Cities and Society*, *62*, 102405. doi:10.1016/j.scs.2020.102405

Madandoust, R., Bazkiyaei, Z. F. Z., & Kazemi, M. (2018). Factor influencing point load tests on concrete. *Asian Journal of Civil Engineering*, *19*(8), 937–947. doi:10.1007/s42107-018-0074-8

Manzano-Agugliaro, F., Montoya, F. G., Sabio-Ortega, A., & García-Cruz, A. (2015). Review of bioclimatic architecture strategies for achieving thermal comfort. *Renewable and Sustainable Energy Reviews*, *49*, 736–755. doi:10.1016/j.rser.2015.04.095

Meteorological Organization Country. (2020). Retrieved March 1, 2020. http:// www.irimo.ir

Mirrahimi, S., Mohamed, M. F., Haw, L. C., Ibrahim, N. L. N., Yusoff, W. F. M., & Aflaki, A. (2016). The effect of building envelope on the thermal comfort and energy saving for high-rise buildings in hot–humid climate. *Renewable and Sustainable Energy Reviews*, *53*, 1508–1519. doi:10.1016/j.rser.2015.09.055

Moein, M. M., Saradar, A., Rahmati, K., Rezakhani, Y., Ashkan, S. A., & Karakouzian, M. (2023). Reliability analysis and experimental investigation of impact resistance of concrete reinforced with polyolefin fiber in different shapes, lengths, and doses. *Journal of Building Engineering*, *69*, 106262. doi:10.1016/j.jobe.2023.106262

Najafi, A., & Pilechiha, P. (2021). *Energy and daylight performance optimization of butterfly inspired intelligent adaptive façade*.

Nigra, M., Lo Verso, V. R. M., Robiglio, M., Pellegrino, A., & Martina, M. (2022). 'Re-coding' environmental regulation – a new simplified metric for daylighting verification during the window and indoor space design process. *Architectural Engineering and Design Management*, *18*(4), 521–544. doi:10.1080/17452007.2021.1941738

Norouziasas, A., Pilehchi Ha, P., Ahmadi, M., & Rijal, H. B. (2022). Evaluation of urban form influence on pedestrians' wind comfort. *Building and Environment*, *224*, 109522. doi:10.1016/j.buildenv.2022.109522

Norouziasas, A., Tabadkani, A., Rahif, R., Amer, M., van Dijk, D., Lamy, H., & Attia, S. (2023). Implementation of ISO/DIS 52016-3 for adaptive façades: A case study of an office building. *Building and Environment*, *235*, 110195. doi:10.1016/j.buildenv.2023.110195

Pilechiha, P., Norouziasas, A., Ghorbani Naeini, H., & Jolma, K. (2021). Evaluation of occupant's adaptive thermal comfort behaviour in naturally ventilated courtyard houses. *Smart and Sustainable Built Environment*, *11*(4), 793–811. doi:10.1108/SASBE-02-2021-0020

Piraei, F., Matusiak, B., & Lo Verso, V. R. M. (2022). Evaluation and optimization of daylighting in heritage buildings: A case-study at high latitudes. *Buildings*, *12*(12), 2045. doi:10.3390/buildings12122045

Pourshaghaghy, A., & Omidvari, M. (2012). Examination of thermal comfort in a hospital using PMV-PPD model. *Applied Ergonomics*, *43*(6), 1089–1095. doi:10.1016/j.apergo.2012.03.010

Rahif, R., Kazemi, M., & Attia, S. (2023). Overheating analysis of optimized nearly Zero-Energy dwelling during current and future heatwaves coincided with cooling system outage. *Energy and Buildings*, *287*, 112998. doi:10.1016/j.enbuild.2023.112998

Rahif, R., Norouziasas, A., Elnagar, E., Doutreloup, S., Pourkiaei, S. M., Amaripadath, D., … Attia, S. (2022). Impact of climate change on nearly zero-energy dwelling in temperate climate: Time-integrated discomfort, HVAC energy performance, and GHG emissions. *Building and Environment*, *223*, 109397. doi:10.1016/j.buildenv.2022.109397

Reilly, A., & Kinnane, O. (2017). The impact of thermal mass on building energy consumption. *Applied Energy*, *198*, 108–121. doi:10.1016/j.apenergy.2017.04.024

Roudsari, M. S., & Pak, M. (2013). Ladybug: A parametric environmental plugin for grasshopper to help designers create an environmentally-conscious design. *Proceedings of BS 2013: 13th Conference of the International Building Performance Simulation Association*, 3128–3135.

Safizadeh, M. (2023). Simulation of the circulation complexity in student residence buildings using space syntax analyses (Case studies: Highland Hall, Rita Atkinson, Rutgers University and Tooker Residences, USA). *Architectural Engineering and Design Management*, *0*(0), 1–20. doi:10.1080/17452007.2023.2203372

Samuelson, H., Claussnitzer, S., Goyal, A., Chen, Y., & Romo-Castillo, A. (2016). Parametric energy simulation in early design: High-rise residential buildings in urban contexts. *Building and Environment*, *101*, 19–31. doi:10.1016/j.buildenv.2016.02.018

Sharma, A., & Kumar, A. (2023). Adaptive thermal comfort of residential buildings in the composite climatic region of India: A field study. *Architectural Engineering and Design Management*, *0*(0), 1–22. doi:10.1080/17452007.2023.2201416

Soflaei, F., Shokouhian, M., Tabadkani, A., Moslehi, H., & Berardi, U. (2020). A simulation-based model for courtyard housing design based on adaptive thermal comfort. *Journal of Building Engineering*, *31*, 101335. doi:10.1016/j.jobe.2020.101335

Talebian, M. H. (2018). *Historic city of yazad World heritage site important, values, management and challenges, IRanina cultural handi craft and tourism organization*.

Taleghani, M. (2018). Outdoor thermal comfort by different heat mitigation strategies- A review. *Renewable and Sustainable Energy Reviews*, *81*(June), 2011–2018. doi:10.1016/j.rser.2017.06.010

Taylor, M., Brown, N. C., & Rim, D. (2021). Optimizing thermal comfort and energy use for learning environments. *Energy and Buildings*, *248*, 111181. doi:10.1016/j.enbuild.2021.111181

Teshnehdel, S., Soflaei, F., & Shokouhian, M. (2020). Assessment of solar shading performance of courtyard houses in desert climate of Kashan, Iran. *Architectural Engineering and Design Management*, *16*(6), 473–492. doi:10.1080/17452007.2020.1758025

Thanu, H. P., Rajasekaran, C., & Deepak, M. D. (2023). Assessing the life cycle performance of green building projects: A building performance score (BPS) model approach. *Architectural Engineering and Design Management*, *19*(4), 378–393. doi:10.1080/17452007.2022.2068495

Tian, W. (2013). A review of sensitivity analysis methods in building energy analysis. *Renewable and Sustainable Energy Reviews*, *20*, 411–419.

US Department of Energy. (2018). *EnergyPlusTM version 8.9.0 documentation: Engineering reference. www.energyplus.net*

Valitabar, M., GhaffarianHoseini, A., GhaffarianHoseini, A., & Attia, S. (2022). Advanced control strategy to maximize view and control discomforting glare: A complex adaptive façade. *Architectural Engineering and Design Management*, 1–21.

Vantyghem, G., Ooms, T., & De Corte, W. (2021). VoxelPrint: A Grasshopper plug-in for voxel-based numerical simulation of concrete printing. *Automation in Construction*, *122*, 103469. doi:10.1016/j.autcon.2020.103469

Wu, Z., Li, N., Wargocki, P., Peng, J., Li, J., & Cui, H. (2019). Field study on thermal comfort and energy saving potential in 11 split air-conditioned office buildings in Changsha, China. *Energy*, *182*, 471–482. doi:10.1016/j.energy.2019.05.204

Yang, H. (2013). The case for being automatic: Introducing the Automatic Linear Modeling (LINEAR) Procedure in SPSS Statistics. *Multiple Linear Regression Viewpoints*, *39*, 27–37.

Yilmaz, N., & Donaldson, A. B. (2005). Consideration of wind barriers for an inner courtyard. *Architectural Engineering and Design Management*, *1*(4), 281–293. doi:10.1080/17452007.2005.9684598

Zaki, S. A., Damiati, S. A., Rijal, H. B., Hagishima, A., & Abd Razak, A. (2017). Adaptive thermal comfort in university classrooms in Malaysia and Japan. *Building and Environment*, *122*, 294–306. doi:10.1016/j.buildenv.2017.06.016

Zhao, J., & Du, Y. (2020). Multi-objective optimization design for windows and shading configuration considering energy consumption and thermal comfort: A case study for office building in different climatic regions of China. *Solar Energy*, *206*, 997–1017. doi:10.1016/j.solener.2020.05.090

Zhou, J., Zhang, G., Lin, Y., & Li, Y. (2008). Coupling of thermal mass and natural ventilation in buildings. *Energy and Buildings*, *40*(6), 979–986. doi:10.1016/j.enbuild.2007.08.001